3 CONTROLLED PROTEOLYTIC DEGRADATION OF PROTEIN-BASED BIOMATERIALS

3.1 Abstract

A new method to easily tailor the proteolytic degradation of protein-based biomaterials is presented. By introducing slight alterations into the primary amino acid sequences of cell-adhesive, elastin-like proteins, the degradation kinetics and resulting patterns of proteolytic fragments are altered. Degradation of protein-polymers containing the VPGIG elastin-like sequence was minimal after 6 h exposure to 0.22 μM elastase (k_{cat} = 0.007 s^{-1}, K_m = 504 μM), while incorporation of lysine residues within this elastin-like domain increased the degradation rate such that no intact protein was present after 6 h exposure (k_{cat} = 0.033 s^{-1}, K_m = 2451 μM). These engineered proteins were crosslinked into freestanding, implantable films with initial elastic moduli ranging from 0.12 - 0.65 MPa. Incorporation of lysine residues within the elastin-like domain resulted in a two-to-sevenfold increase in the bulk material degradation rate compared to the VPGIG elastin-like protein. These results demonstrate the usefulness of protein engineering to create new cell-adhesive biomaterials with tunable initial moduli and degradation properties.

Manuscript prepared for submission by Sarah C. Heilshorn[1], Paul J. Nowatzki[1], Tetsuji Yamaoka[2], David A. Tirrell[1]

(1) Division of Chemistry and Chemical Engineering, California Institute of Technology

(2) Department of Polymer Science and Engineering, Kyoto Institute of Technology

3.2 Introduction

The ability to tailor the degradation rate of implanted biomaterials is a necessity when designing materials for specific medical uses. In traditional synthetic biomaterials, a variety of strategies have been employed to control degradation rates. These include optimization of polymer chemistry to alter the concentration of hydrolysable bonds,[1-3] blending of polymer crosslink units to control network structure,[4] and inclusion of peptides into a synthetic polymer network to promote sequence-specific degradation by matrix metalloproteinases.[5] In this work, we employ a genetic engineering approach to design protein-based biomaterials with tailored proteolytic degradation rates.

Engineered proteins are an attractive class of biomedical materials due to their templated biosynthesis, which allows precise control of molecular architecture. This strategy has been utilized in the *de novo* design of artificial proteins exhibiting a variety of novel structural and biomimetic properties.[6-11] Artificial proteins containing elastin-like repeats are of particular interest due to their high expression levels, ease of purification,[12] biocompatibility,[13] and tunable mechanical properties.[14-16] By judicious placement of crosslinking sites, the elastic modulus of the resulting bulk biomaterial can be controlled within the range of 0.1-1.0 MPa.

To promote cell interactions with these biomaterials, various cell-binding and cell-signaling domains have been interspersed with the elastin-like structural units.[17-21] Incorporation of the CS5 domain into these elastin-like polymers promotes sequence-specific spreading and adhesion of human umbilical vein

endothelial cells (HUVEC).[18,22] These materials exhibit many of the characteristics desirable for use as small-diameter vascular grafts, including elasticity similar to natural blood vessels and adhesion of endothelial cells.

Numerous enzymes with proteolytic capabilities exist *in vivo*; however, native elastin is resistant to many of these proteases, with the notable exception of elastase.[23] Therefore, this study seeks to quantify the elastase degradation of engineered elastin-like materials and develop strategies by which this degradation rate can be altered. Two forms of elastase are commonly found in humans, pancreatic elastase and leukocyte elastase (HLE, also known as lysosomal elastase, granulocyte elastase, polymorphonuclear elastase, and neutrophil elastase), which differ in substrate specificity and inhibitor sensitivity. HLE preferentially cleaves the peptide bond directly following small, hydrophobic amino acid side chains.[24] Elastase activity is greatly affected by enzyme-substrate contacts remote from the active site.[25,26] This suggests that appropriate genetic engineering of the elastin-like repeat within engineered protein-polymers would allow tuning of HLE degradation rates. Indeed, a comparison of HLE degradation of protein-polymers containing two distinct elastin-like sequences (Figure 3.1) resulted in different patterns of proteolytic fragments and a large difference in the rate of bulk material degradation. This change in degradation was caused by insertion of lysine residues into the elastin-like sequence while maintaining the authenticity of the CS5 cell-binding domain. Therefore, a protein-design strategy has been validated as a novel method to control degradation rates of protein-based, cell-adhesive biomaterials.

Protein aE1

M MASMTGGQQMG HHHHHHH DDDDK {LD GEEIQIGHIPREDVDYHLYP G [(VPGIG)$_2$VPGKG(VPGIG)$_2$]$_4$ }$_3$ LE
T7 tag *His tag* *CS5 cell-binding domain* *elastin-like domain*

Mol Wt. = 37.1 kDa; expected fragments = multiples of 1.3, 1.7, and 3.7 kDa

Protein aE2

M MASMTGGQQMG RKTMG {LD GEEIQIGHIPREDVDYHLYP G [VPGIG]$_{25}$ VP}$_3$ LEKAAKLE
T7 tag *CS5 cell-binding domain* *elastin-like domain*

Mol. Wt. = 43.0 kDa; expected fragments = 2.6, 13.4, 16.0, 26.9, 29.5, and 38.1 kDa

Protein aE3

M MASMTGGQQMG RKTMG {LD GEEIQIGHIPREDVDYHLYP G [VPGIG]$_{25}$ VP}$_3$ LEKAAKLE
T7 tag *CS5 cell-binding domain* *elastin-like domain*

Mol. Wt. = 16.1 kDa (fragmentation not analyzed – crosslinked films only)

Figure 3.1 Amino acid sequences of the engineered elastin-like proteins. Protein aE1 has three repeats of the CS5 and lysine-containing elastin-like domains. Protein aE2 has three repeats of the CS5 and elastin-like domains with lysine residues at the C- and N-termini only. Protein aE3 is identical to aE2 except it contains only one repeat, decreasing the molecular weight between the lysine residues at the C- and N-termini. The preferred elastase cleavage sites, based on N-terminal sequencing of proteolytic fragments (Table 3.1), are identified by arrows. Cleavage at these sites would result in the listed fragment mass sizes.

3.3 Experimental

3.3.1 Protein expression and purification.

Plasmids encoding sequences aE1, aE2, and aE3 have been previously described.[14,15] Proteins were expressed in *E. coli* and purified as reported.[18] Purity was assessed by SDS-PAGE and Western blotting with anti-T7 tag-horseradish peroxidase conjugate antibody (Novagen).

3.3.2 Analysis of elastase degradation fragments.

The degradation reaction was carried out at 37°C for 3 days in sodium borate buffer, pH 8, with 0.22 μM human leukocyte elastase (HLE, Elastin Products Company, Owensville, MO) and 100 μM protein aE1 or aE2. Samples were taken at 0, 1, 3, 6, 12, 24, 48, and 72 h and diluted with an equal amount of 2X SDS-sample buffer including β-mercaptoethanol and frozen at -20°C. Samples were boiled for 5 min and run on a 12% Tris-tricine gel at 150 V for 1 h. Gels were run in triplicate and either stained with Coomassie blue, transferred to PVDF membrane for N-terminal sequencing of proteolysis fragments, or transferred to nitrocellulose for Western blot analysis using an anti-T7 tag-horseradish peroxidase conjugate antibody. Densitometry was performed on Western blots using Image J (NIH freeware image analysis program) to quantify the amount of whole-length protein remaining at each time point, as compared to known whole-length protein concentrations. N-terminal sequencing by Edman degradation was performed on proteolysis fragments at the California

Institute of Technology Protein/Peptide Micro Analytical Laboratory using a protein micro-sequencer (Applied Biosystems, model 492).

3.3.3 Kinetics of elastase degradation.

The degradation reaction was carried out at 37°C for 6 h in sodium borate buffer, pH 8, with 0.22 μM HLE and 5-108 μM protein under constant mixing. The extent of reaction was characterized using 2,4,6-trinitrobenzene sulfonic acid at 4°C to quantify the number of N-termini in solution at 0, 1, 2, 4, and 6 hours. Six replicates of each substrate concentration were performed.

3.3.4 Crosslinking of protein films.

To crosslink proteins aE1 and aE2, 30 mg of protein was dissolved in 250 μL of water at 4°C, and tris-succinimidyl aminotriacetate (TSAT) was dissolved in 50 μL of 25:75 dimethylformamide:dimethyl sulfoxide at 4°C. The two solutions were rapidly mixed and pipetted into an open-faced mold. Films were dried overnight at 55°C. To achieve similar elastic moduli between the two films, a 0.35:1 ratio of succinimidyl ester functional groups to primary amines was used to crosslink aE, while a 1:1 ratio was used for aE3.

Matching previous work, aE2 was crosslinked with hexamethylene diisocyanate (HMDI) in dimethylsulfoxide,[16] and aE1 was crosslinked with bis(sulfosuccinimidyl) suberate (BS3) in 4°C water.[15] The crosslinker concentrations were chosen such that each film had an initial elastic modulus of ~0.6 MPa, similar to that of native elastin.[27] For aE1, the ratio of succinimidyl

ester groups in BS3 to primary amines in the protein was 1:1; for aE2, a 5:1 stoichiometric ratio of isocyanates to primary amines was used.

3.3.5 Elastase degradation of crosslinked films.

Crosslinked films (~3 mg dry, approximate dimensions = 0.25 x 1.5 x 12 mm) were exposed to 0.5 mL of 0.22 μM elastase in PBS solution at 37°C. At various time points, samples were removed, equilibrated for 15 min in PBS (pH 7.4, 37°C), and tensile tested with a modified Instron instrument (model 5542). Samples were extended 20% at a rate of 10% gauge length/min; at this slow rate and minimal extension, viscoelastic effects and hysteresis were observed to be negligible. The elastic moduli were calculated over the initial portion (0-4%) of the stress-strain curves. The samples did not noticeably swell or shrink during the course of the experiment, so the initial cross-sectional area of each sample was used to calculate stress at all time points.

3.3.6 Weight fraction protein.

Protein content of the films was determined from the mass difference between wet and dry samples. Wet samples were prepared by equilibration in PBS, pH 7.4, 37°C, followed by wicking away of excess buffer with filter paper. Films were dried at 50°C for 12 hours in a vacuum oven.

3.4 Results and Discussion

3.4.1 Protein expression and purification.

The purification takes advantage of the differential solubility of elastin-like proteins above and below a lower critical solution temperature. Thermal cycling and centrifugation was used to purify proteins aE1, aE2, and aE3 in yields of 2.6, 6.6, and 2.1 g, respectively, from 10 L batch fermentations, which correspond to expression yields of 10, 22, and 7 mg/g wet cell mass.

3.4.2 Elastase degradation of engineered proteins with altered elastin-like sequences.

The pattern of proteolytic fragments formed during HLE degradation was analyzed by SDS-PAGE and is shown in Figure 3.2; the number of fragments versus time is indicated in Figure 3.3. To simulate physiologically relevant conditions, the degradation reaction was performed at 37°C, above the LCST for both proteins. As expected, the variations in amino acid sequence within the elastin-like domains altered HLE degradation of the two synthetic proteins. HLE degradation of protein aE1 resulted in many smaller bands of fragments after only 1 h of elastase exposure and complete protein degradation at 12 h. In contrast, degradation of protein aE2 resulted in six primary fragments, approximately 3, 12, 15, 27, 30, and 38 kD in mass, and complete protein degradation at 72 h. Therefore, both the time course of degradation and the resulting molecular weights of proteolytic fragments can be altered by replacing the lysine residues within the elastin-like domain of protein aE1 with isoleucine residues in protein aE2.

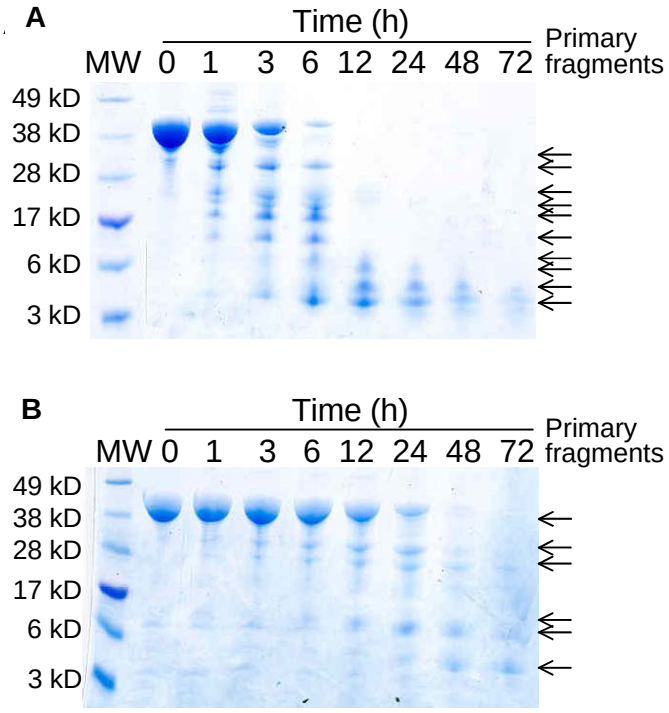

Figure 3.2 SDS-PAGE of elastase degradation fragments of proteins aE1 (A) and aE2 (B). Protein aE1 is degraded into several fragments that form a "ladder" of molecular weights, denoted by the arrows to the right. Protein aE2 degrades into six fragments with approximate molecular weights of 3, 12, 15, 27, 30, and 38 kD, again denoted by the arrows. These fragment sizes correspond to the predicted proteolytic fragment molecular weights in Figure 3.1.

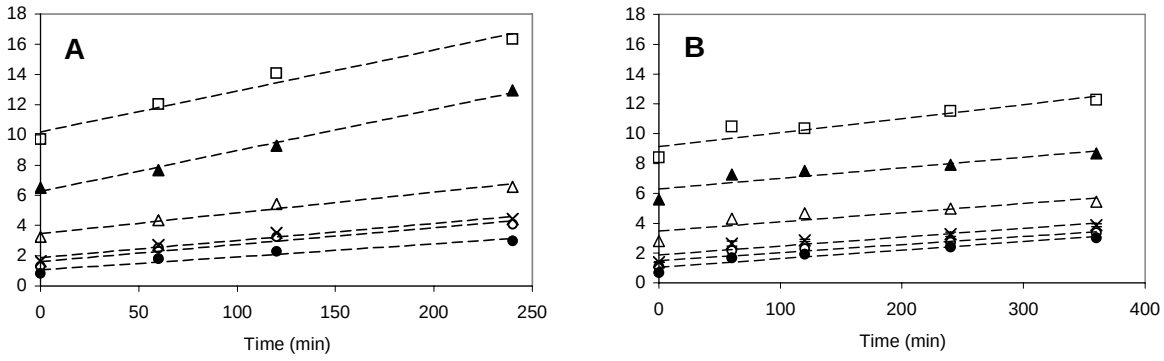

Figure 3.3 Number of N-termini detected at each time point for proteins aE1 (A) and aE2 (B). Protein concentrations for A are 108, 72, 36, 18, 14, and 9 μM (descending). Protein concentrations for B are 93, 62, 31, 16, 12, and 6 μM.

N-terminal sequencing of several degradation bands revealed that the peptide bond after isoleucine was the favored cut-site of both proteins aE1 and aE2 (Table 3.1). Although synthetic peptide studies have suggested that valine is the optimum cut-site for HLE, other side chains including alanine, methionine, leucine, isoleucine, and threonine have been reported, as have the artificial amino acids norvaline and norleucine.[26,28,29] Protein aE1 appeared to cleave preferentially at the isoleucines contained within the elastin-like sequences, resulting in many degradation fragments varying in size by one elastin-unit repeat. In contrast, protein aE2 was preferentially cleaved at the isoleucines contained within the CS5 cell-binding domains. Based on the N-terminal sequencing results, the cleavage sites and the molecular weight patterns of proteolytic fragments for proteins aE1 and aE2 were predicted (Figure 3.1).

Table 3.1 N-terminal sequencing results of selected proteolytic fragments.

Protein	Fragment size (kD)	Called sequence	Protein region of the called sequence	N-terminal cut site of the called sequence
aE1	28	GVPGIG	Elastin-like domain	Isoleucine
	28	MMASM	N-terminus	Not applicable
	21	GVPGI	Elastin-like domain	Isoleucine
	17	GVPGIG	Elastin-like domain	Isoleucine
	17	MMASM	N-terminus	Not applicable
aE2	15	MMASM	N-terminus	Not applicable
	12	GHIPRE	CS5 domain	Isoleucine

Consistent with the hypothesis that protein aE1 is cleaved at multiple sites within the elastin-like domain, Figure 3.3A contains a "ladder" of proteolytic fragment sizes. Similarly, the predicted fragment sizes of protein aE2 match well with the bands in Figure 3.3B.

It has previously been found that, owing to the high content of hydrophobic amino acids in the elastin-like domain, various protein fragments stain with Coomassie blue very differently depending on the presence or absence of the T7 tag (unpublished data). Therefore, Western analysis was used to determine the amount of full-length, intact protein remaining after HLE exposure for various times (Figure 3.4A). Densitometry was employed to quantify the percent of full-length protein remaining at each time point (Figure 3.4B). At 6 h, 0% of protein aE1 remained intact compared to over 90% of protein aE2. The reaction velocity is constant for both reactions, although protein aE2 degrades over a much longer time scale than protein aE1. This suggests that the protein concentration for each reaction is saturating, i.e., the substrate concentration is much higher than the Michaelis constant (K_m), and the reaction rates are at their maximum velocities. (This assumption is validated by more rigorous kinetic testing below; see Figure 3.5.) Therefore, the approximate degradation rate constant, k_{cat}, is 0.036 s^{-1} for protein aE1 and 0.003 s^{-1} for protein aE2.

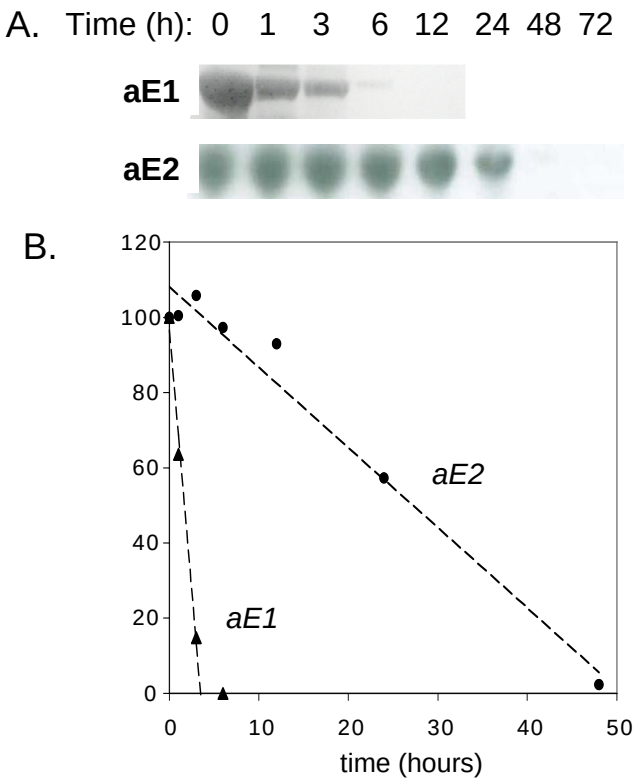

Figure 3.4 (A) Western blot of full-length, intact proteins aE1 and aE2 remaining after HLE exposure. (B) Full-length protein aE1 and aE2 remaining after HLE exposure at various time points.

A more rigorous kinetic analysis was performed using 2,4,6-trinitrobenzene sulfonic acid to determine the kinetic constants of the degradation reaction (Figure 3.5). Similar to the results above, constant initial reactions rates were found for both proteins aE1 and aE2 at each substrate concentration tested. The relationship between initial reaction rate and substrate concentration for both proteins aE1 and aE2 fit the Michaelis-Menten enzyme kinetic model, yielding coefficients of determination, i.e., R-values, of 0.95 and 0.77, respectively. Because of the slow degradation of protein aE2, the data had a lower signal-to-noise ratio and thus more uncertainty was introduced into the

parameter fitting. Nevertheless, the determined k_{cat} values of 0.033 s^{-1} and 0.007 s^{-1} for proteins aE1 and aE2, respectively, are in good agreement with the degradation rate constants calculated using the densitometry method described above.

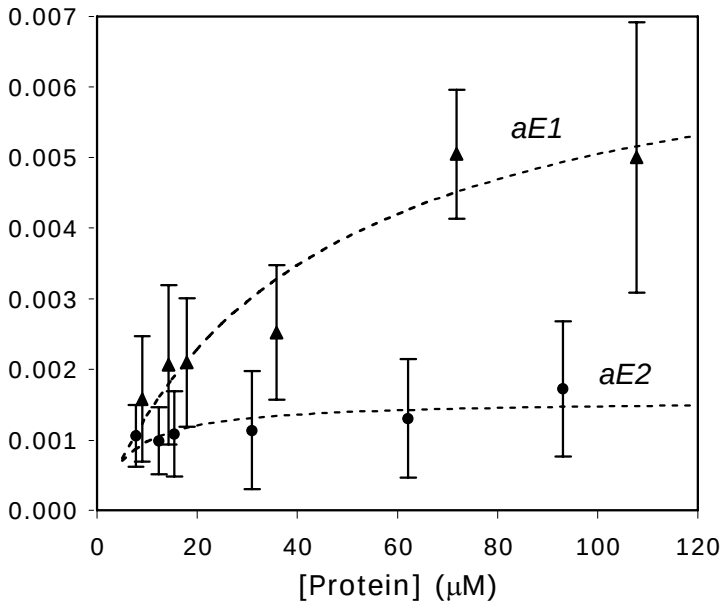

Figure 3.5 Kinetic analysis of elastase degradation of proteins aE1 and aE2. Error bars represent a 90% confidence interval. Dashed lines represent best fits of the observed data to the Michaelis-Menten model.

Because the molecular weight (aE1=37,100 Da, aE2=43,000 Da) and isoleucine content (aE1=57 residues/chain, aE2=84 residues/chain) of each protein are different, Michaelis constant (K_m) values were determined both as a function of total protein concentration ($K_{m,bulk}$), which is relevant for bulk material degradation, and isoleucine concentration ($K_{m,Ile}$), which is relevant for comparison of reaction rates. For protein aE1, $K_{m,bulk}$ is 43 μM and $K_{m,Ile}$ is

2.45 mM. For the slower degrading protein aE2, $K_{m,bulk}$ is 6 μM and $K_{m,Ile}$ is 0.50 mM. Interestingly, $k_{cat}/K_{m,Ile}$, a measure of the enzyme's "kinetic perfection,"[30] is similar for both reactions (aE1=13.5 $s^{-1}M^{-1}$, aE2=13.9 $s^{-1}M^{-1}$). Therefore, at substrate concentrations much lower than $K_{m,bulk}$, the two proteins will degrade at similar rates; however, at higher substrate concentrations, which are required for freestanding, implantable films as described later (Figure 3.6), the maximal degradation velocities of the two proteins are markedly different.

The time required for the reaction to occur was qualitatively similar to those published in the literature for elastase degradation of elastin and much longer than the times required for the synthetic peptide substrate reactions.[28,31-33] However, these reports did not analyze the kinetic constants of the degradation of insoluble elastin. Kinetic constants for HLE degradation of plasmin have been reported using an indirect competitive reaction method to measure K_m and a direct turbidimetric method to measure k_{cat}. These data report a K_m value (0.442 μM) much lower than that of proteins aE1 and aE2 and a k_{cat} value (0.022 s^{-1}) similar to protein aE1.[34] Meanwhile, the K_m and k_{cat} values reported for HLE degradation of soluble synthetic peptide substrates vary from 140-160,000 μM and 0.01-37 s^{-1}, respectively, depending on amino acid sequence.[25,28]

3.4.3 Elastase degradation of crosslinked protein films.

Next, freestanding films of the crosslinked proteins were exposed to HLE to determine if the degradation rates of bulk protein-based biomaterials were similarly altered by changes in the primary amino acid sequence. Use of the trifunctional crosslinker molecule tris-succinimidyl aminotriacetate (TSAT) allowed at different ratios for aE1 and aE3 allowed the initial elastic moduli (and thus the molecular weight between crosslinks), water content, and dimensions of the films being compared to be similar; physical properties of the films are listed below in Table 3.2. By substituting the lower-molecular weight protein aE3 for the architecturally identical protein aE2 in the films, a smaller molecular weight between crosslinks (M_c), and thus a higher elastic modulus (E) similar to protein aE1 could be achieved.

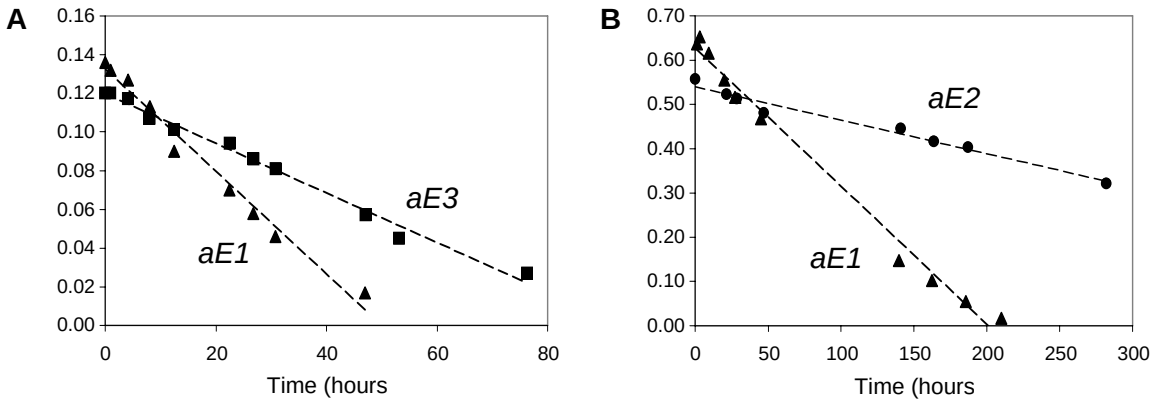

Figure 3.6 (A) Decrease in elastic modulus after HLE exposure of protein films aE1 (triangles) and aE3 (squares) formed with TSAT crosslinking chemistry. (B) Decrease in elastic modulus after HLE exposure of crosslinked protein films aE1 (triangles) and aE2 (circles) formed with differing crosslinking chemistries to yield high initial moduli.

Table 3.2 Properties and degradation rates of crosslinked elastin-like protein films.

Protein	Crosslinker / stoichiometry	Weight fraction polymer	Sample polymer mass (mg)	E_o (MPa)	M_c initial (kDa/mol)	Degradation rate constant (s^{-1})
aE1	TSAT 0.35×	0.35	2.8	0.136	25.9	0.0058
aE3	TSAT 1.0×	0.37	2.6	0.120	31.0	0.0022
aE1	BS3 1×	0.52	4.0	0.65	8.0	0.0110
aE2	HMDI 5×	0.73	2.6	0.56	13.1	0.0015

As expected, films of protein aE3 degraded significantly faster than did films of protein aE1 (Figure 3.6A), reflecting the results for the soluble proteins. If it is assumed that these films behave like ideal networks and that the substrate concentration is saturating, an approximate first-order rate constant of degradation can be determined. The substrate concentration for each film listed in Table 3.2 is greater than 10 mM, which is about three orders of magnitude larger than the $K_{m,bulk}$ values determined from Figure 3.5. Similarly, the protein concentration required for a variety of biomedical applications such as tissue engineering scaffolds, drug-delivery vehicles, or implanted materials for tissue reconstruction would presumably be much larger than $K_{m,bulk}$. Therefore, the degradation reaction will proceed at maximal velocity. HLE is assumed to diffuse freely into the water-rich, highly mobile elastin-like networks; the observed uniformity of degradation throughout the film cross-section, as opposed to degradation only at the film surfaces, supports this assumption. Prior work with these [14-16] and other elastin-like proteins[35] have shown that the ideal network assumption is a reasonable one. For an ideal rubber network,

$E=3\rho RT/M_c$, where E is the elastic modulus, ρ is the polymer density (taken to be 1.3 g/ml,[36] multiplied by the appropriate volume fraction polymer from Table 3.2), T is the temperature, and M_c is the molecular weight between effective crosslinks.[37] The molar concentration of effective crosslinks can then be calculated from the total dry film mass divided by M_c. As the film is degraded, the concentration of effective crosslinks is reduced; therefore, the maximal degradation velocity is defined as the loss in effective crosslinks over time. The effective degradation rate constants are listed in Table 3.2 above. Because some peptide cleavages will not result in loss of an effective crosslink, the degradation rate constants calculated from this analysis are smaller than the k_{cat} values determined above. Analogously to the degradation rates of uncrosslinked proteins, the insertion of lysine residues into the elastin-like domains resulted in quicker bulk film degradation.

The difference in degradation rates is also apparent when comparing films of much higher initial elastic moduli (Figure 3.6B), although the comparison is less straightforward because the crosslinker and water content are different. Films of protein aE1 and protein aE2, crosslinked with bis(sulfosuccinimidyl suberate) (BS3) and hexamethylene diisocyanate (HMDI), respectively, were previously characterized as having initial elastic moduli near 0.6 MPa, typical of native elastin.[15,16,27] Film aE1 displayed an effective degradation rate constant 7.3 times larger than film aE2 (Table 1). Taken together, these results demonstrate that crosslinked films of elastin-like engineered proteins can be designed to have a variety of initial moduli and HLE degradation rates.

3.4.4 Elastase concentration considerations.

It is important to note that the HLE concentration used in these experiments was chosen somewhat arbitrarily based on previous studies analyzing degradation kinetics of synthetic substrates. The HLE level chosen, 6.3 μg/ml or 0.22 μM, resulted in degradation rates easily quantified over short time scales, i.e., hours and days. This allowed the facile comparison of elastase degradation through design of the elastin-like sequence. Clinical studies cite HLE levels of 53.3 ± 9.3 ng/ml in human plasma.[38] Furthermore, HLE activity is tightly regulated *in vivo* by natural inhibitors; therefore, the same concentration of purified HLE will display much higher activity *in vitro*.[39] Further complicating this matter, serum levels of HLE are thought to increase in response to sepsis and procedures requiring cardiopulmonary bypass.[40,41] For these reasons, future analyses of degradation rates of engineered proteins for specific medical applications will be most instructive if evaluated *in vivo*. This work represents a first step in establishing the kinetics and time-scales of elastase degradation and validates the genetic engineering approach as a novel method to tailor substrate degradability.

3.5 Conclusions

This study demonstrates the usefulness of a novel genetic engineering method to synthesize biomaterials with controlled degradation rates for potential medical applications. Two synthetic proteins containing identical cell-binding domains were shown to exhibit altered patterns of HLE degradation based on the amino acid sequence engineered within the elastin-like domain. Insertion of lysine residues into the elastin-like domain resulted in a bulk, crosslinked film with an effective degradation rate constant 2.6 to 7.3 times larger than films without lysines in the elastin-like domains. Through variation in the conditions of crosslinking and genetic engineering of the molecular weight between crosslinks, the moduli of elastin-like synthetic protein films can also be tailored. Control over the initial modulus and degradation rate along with the ability to include cell-recognition domains within the synthetic proteins suggest these materials may be useful in designing tissue engineering scaffolds, drug-delivery vehicles, or implanted materials for tissue reconstruction.

Acknowledgments

This work was supported by NIH Grant 5 ROI HL59987-03, NSF Grant BES-9901648, and the NSF East Asia Summer Institute. N-terminal sequencing was performed by the Caltech Protein/Peptide Microanalytical Laboratory and supported by The Beckman Institute at Caltech.

3.6 References

(1) Elbert DL, Hubbell JA. Conjugate addition reactions combined with free-radical cross-linking for the design of materials for tissue engineering. *Biomacromolecules* **2001**, *2*, 430-441.

(2) Davis KA, Burdick JA, Anseth KS. Photoinitiated crosslinked degradable copolymer networks for tissue engineering applications. *Biomaterials* **2003**, *24*, 2485-2495.

(3) Kim BS, Hrkach JS, Langer R. Biodegradable photo-crosslinked poly(ether-ester) networks for lubricious coatings. *Biomaterials* **2000**, *21*, 259-265.

(4) Rydholm AE, Bowman CN, Anseth KS. Degradable thiol-acrylate photopolymers: polymerization and degradation behavior of an in situ forming biomaterial. *Biomaterials* **2005**, *26*, 4495-4506.

(5) Lutolf MP, Lauer-Fields JL, Schmoekel HG, Metters AT, Weber FE, Fields GB, Hubbell JA. Synthetic matrix metalloproteinase-sensitive hydrogels for the conduction of tissue regeneration: Engineering cell-invasion characteristics. *Proc. Natl. Acad. Sci. U. S. A.* **2003**, *100*, 5413-5418.

(6) McPherson DT, Xu J, Urry DW. Product purification by reversible phase transition following Escherichia coli expression of genes encoding up to 251 repeats of the elastomeric pentapeptide GVGVP. *Protein Expr. Purif.* **1996**, *7*, 51-57.

(7) Petka WA, Harden JL, McGrath KP, Wirtz D, Tirrell DA. Reversible hydrogels from self-assembling artificial proteins. *Science* **1998**, *281*, 389-392.

(8) Krejchi MT, Atkins EDT, Waddon AJ, Fournier MJ, Mason TL, Tirrell DA. Chemical sequence control of beta-sheet assembly in macromolecular crystals of periodic polypeptides. *Science* **1994**, *265*, 1427-1432.

(9) Szela S, Avtges P, Valluzzi R, Winkler S, Wilson D, Kirschner D, Kaplan DL. Reduction-oxidation control of beta-sheet assembly in genetically engineered silk. *Biomacromolecules* **2000**, *1*, 534-542.

(10) O'Brien JP, Fahnestock SR, Termonia Y, Gardner KCH. Nylons from nature: Synthetic analogs to spider silk. *Adv. Mater.* **1998**, *10*, 1185-1195.

(11) Meyer DE, Chilkoti A. Genetically encoded synthesis of protein-based polymers with precisely specified molecular weight and sequence by recursive directional

ligation: Examples from the elastin-like polypeptide system. *Biomacromolecules* **2002**, *3*, 357-367.

(12) Urry DW, Gowda DC, Parker TM, Luan CH, Reid MC, Harris CM, Pattanaik A, Harris RD. Hydrophobicity scale for proteins based on inverse temperature transitions. *Biopolymers* **1992**, *32*, 1243-1250.

(13) Urry DW, Parker TM, Reid MC, Gowda DC. Biocompatibility of the bioelastic materials, poly(GVGVP) and its gamma-irradiation cross-linked matrix - summary of generic biological test-results. *J. Bioactive and Compatible Polym.* **1991**, *6*, 263-282.

(14) Welsh ER, Tirrell DA. Engineering the extracellular matrix: A novel approach to polymeric biomaterials. I. Control of the physical properties of artificial protein matrices designed to support adhesion of vascular endothelial cells. *Biomacromolecules* **2000**, *1*, 23-30.

(15) Di Zio K, Tirrell DA. Mechanical properties of artificial protein matrices engineered for control of cell and tissue behavior. *Macromolecules* **2003**, *36*, 1553-1558.

(16) Nowatzki PJ, Tirrell DA. Physical properties of artificial extracellular matrix protein films prepared by isocyanate crosslinking. *Biomaterials* **2004**, *25*, 1261-1267.

(17) Nicol A, Gowda DC, Urry DW. Cell-adhesion and growth on synthetic elastomeric matrices containing Arg-Gly-Asp-Ser-3. *J. Biomed. Mater. Res.* **1992**, *26*, 393-413.

(18) Heilshorn SC, DiZio KA, Welsh ER, Tirrell DA. Endothelial cell adhesion to the fibronectin CS5 domain in artificial extracellular matrix proteins. *Biomaterials* **2003**, *24*, 4245-4252.

(19) Panitch A, Yamaoka T, Fournier MJ, Mason TL, Tirrell DA. Design and biosynthesis of elastin-like artificial extracellular matrix proteins containing periodically spaced fibronectin CS5 domains. *Macromolecules* **1999**, *32*, 1701-1703.

(20) Liu CY, Apuzzo MLJ, Tirrell DA. Engineering of the extracellular matrix: Working toward neural stem cell programming and neurorestoration - Concept and progress report. *Neurosurgery* **2003**, *52*, 1154-1165.

(21) Liu JC, Heilshorn SC, Tirrell DA. Comparative cell response to artificial extracellular matrix proteins containing the RGD and CS5 cell-binding domains. *Biomacromolecules* **2004**, *5*, 497-504.

(22) Heilshorn SC, Liu JC, Tirrell DA. Cell-binding domain context affects cell behavior on engineered proteins. *Biomacromolecules* **2005**, *6*, 318-323.

(23) Robert L, Robert AM, Jacotot B. Elastin-elastase-atherosclerosis revisited. *Atherosclerosis* **1998**, *140*, 281-295.

(24) Geneste P, Bender ML. Esterolytic activity of elastase. *Proc. Natl. Acad. Sci. U. S. A.* **1969**, *64*, 683-685.

(25) Thompson RC, Blout ER. Dependence of kinetic parameters for elastase-catalyzed amide hydrolysis on length of peptide substrates. *Biochemistry* **1973**, *12*, 57-65.

(26) Harper JW, Cook RR, Roberts CJ, McLaughlin BJ, Powers JC. Active-site mapping of the serine proteases human leukocyte elastase, cathepsin G, porcine pancreatic elastase, rat mast-cell protease-I and protease-II, bovine chymotrypsin-A-alpha, and staphylococcus-aureus protease V-8 using tripeptide thiobenzyl ester substrates. *Biochemistry* **1984**, *23*, 2995-3002.

(27) Abbott WM, Cambria RP *Biologic and Synthetic Vascular Prostheses*; Gurne & Stratton: New York, **1982**.

(28) Nakajima K, Powers JC, Ashe BM, Zimmerman M. Mapping the extended substrate binding-site of cathepsin-G and human-leukocyte elastase - studies with peptide substrates related to the alpha-1-protease inhibitor reactive site. *J. Biol. Chem.* **1979**, *254*, 4027-4032.

(29) McBride JD, Freeman HNM, Leatherbarrow RJ. Selection of human elastase inhibitors from a conformationally-constrained combinatorial peptide library. *Eur. J. Biochem.* **1999**, *266*, 403-412.

(30) Stryer L *Biochemistry*; 4 ed.; W. H. Freeman and Company: New York, **1995**.

(31) Rao SK, Mathrubutham M, Karteron A, Sorensen K, Cohen JR. A versatile microassay for elastase using succinylated elastin. *Anal. Biochem.* **1997**, *250*, 222-227.

(32) Reilly CF, Travis J. Degradation of human-lung elastin by neutrophil proteinases. *Biochim. Biophys. Acta* **1980**, *621*, 147-157.

(33) Morrison HM, Welgus HG, Owen CA, Stockley RA, Campbell EJ. Interaction between leukocyte elastase and elastin: quantitative and catalytic analyses. *Biochim. Biophys. Acta - Prot. Struct. Mol. Enzymol.* **1999**, *1430*, 179-190.

(34) Kolev K, Komorowicz E, Owen WG, Machovich R. Quantitative comparison of fibrin degradation with plasmin, miniplasmin, neurophil leukocyte elastase and cathepsin G. *Thromb. Haemost.* **1996**, *75*, 140-146.

(35) Aaron BB, Gosline JM. Elastin as a random network elastomer - a mechanical and optical analysis of single elastin fibers. *Biopolymers* **1981**, *20*, 1247-1260.

(36) Gosline J, Lillie M, Carrington E, Guerette P, Ortlepp C, Savage K. Elastic proteins: biological roles and mechanical properties. *Philos. Trans. R. Soc. Lond. B Biol. Sci.* **2002**, *357*, 121-132.

(37) Aklonis JJ *Introduction to Polymer Viscoelasticity*; Wiley-Interscience: New York, **1983**.

(38) Oudijk EJD, Nieuwenhuis HK, Bos R, Fijnheer R. Elastase mediated fibrinolysis in acute promyelocytic leukemia. *Thromb. Haemost.* **2000**, *83*, 906-908.

(39) Hornebeck W, Potazman JP, Decremoux H, Bellon G, Robert L. Elastase-type activity of human serum - its variation in chronic obstructive lung diseases and atherosclerosis. *Clin. Physiol. Biochem.* **1983**, *1*, 285-292.

(40) Mojcik CF, Levy JH. Aprotinin and the systemic inflammatory response after cardiopulmonary bypass. *Ann. Thorac. Surg.* **2001**, *71*, 745-754.

(41) Gohra H, Mikamo A, Okada H, Hamano KI, Zempo N, Esato K. Granulocyte elastase release and pulmonary hemodynamics in patients with mitral valvular disease. *World J. Surg.* **2002**, *26*, 643-647.